Cages, Baskets, Ladders, and Tubes: Conformational Studies of Polyhedral Oligomeric Silsesquioxanes

Sean D. Hillson,[†] Emelyn Smith,[†] Martel Zeldin,[‡] and Carol A. Parish*[,‡]

Department of Chemistry, University of Richmond, Richmond, Virginia 23173

Received: June 2, 2005; In Final Form: July 27, 2005

The conformational flexibility of a series of cage, basket, ladder, and tube polyhedral oligomeric silsesquioxanes (POSS) has been examined using the Low Mode:Monte Carlo conformational search method in conjunction with the MM3*/GBSA($CHCl_3$) surface. An ensemble of low energy structures was generated and used to explore the molecular shape and flexibility of each system. The results indicate that, except for the ladder molecule, the incompletely condensed systems that are studied are relatively rigid. Even in cases where the molecule is able to adopt numerous low energy conformations, the overall shape remains cage-like and the conformations differ only by small angles or substituent orientations. The ladder molecule is the most flexible and this ensemble clusters into two families: one that is cage-like and the other that is more open and ladder-like. The conformational flexibilities in the gas and solvent phases, as approximated using the GBSA continuum solvent model, are very similar.

Introduction

Silicious materials (e.g., amorphous silica) are well-known commercially as fillers, absorbents, and solid-phase immobilized supports for heterogeneous catalysis.[1−4] Polyhedral oligomeric silsesquioxanes (POSS), which are a class of molecular species that comprise polyhedral cages (**1**), partial (open) cages (**2**), tubes (**3**), 2-dimensional ladders (**4**), and random extended network structures, have been utilized as oligomeric siloxane models of amorphous silica.[5] Although silsesquioxanes were recognized more than a half-century ago,[6] it was not until the development of rational synthetic methodologies, mainly sol−gel techniques, that many of these compounds containing a wide variety of substituents (R = organic, H−, HO−) were prepared in high yield and structurally characterized.[7−12] A plethora of these materials are now available commercially through Hybrid Plastics.[13] As a result, there is active research and a rapidly growing literature on the applications of these oligomeric siloxanes containing Si atoms capped with organic-functional substituents, organometallic moieties, and hydroxide. Owing to their exceptional thermal−mechanical properties and oxidative stability, a number of these compounds are used as ceramics fillers and are incorporated into inorganic−organic hybrid copolymers that have diverse applications in electronics devices,[14] as coating films,[15] and in lithography.[16]

Unlike amorphous silica, silsesquioxanes can now be prepared with organic substituents (R) that can improve solubility in protic and aprotic solvents.[5,17−23] In addition, these materials also possess catalytic activity. Kudo and Gordon reported an ab initio electronic treatment of the catalytic reactivity of titanium-containing polyhedral (T_8) oligomeric silsesquioxanes toward olefin oxidation by peroxides. They predicted an increase in reactivity as the number of titanium atoms in the cage increases.[24] Duchateau et al. used boron-, aluminum-, and gallium-containing silsesquioxanes as homogeneous catalyst models of silica for group 13 element zeolite and silicate heterogeneous catalysts.[25]

Our interest in catalytically active POSS stems from the reports by Fife et al.[26,27] and Gorenstein et al.,[28] who have demonstrated that water-soluble oligomeric siloxanes with catalytically active dialkylaminopyridinyl moieties are *p*-nitrophenylesterases with remarkable substrate specificity owing to a strong binding interaction between a siloxane pocket and the lipophilic substrate. We are interested in silsesquioxanes, particularly the open cages, tubes, and ladders, as homogeneous and heterogeneous catalysts because of their hydrophobicity and potential for providing binding sites—pockets or surfaces—for catalytic conversions of reactive organic lipophiles. While there have been numerous theoretical studies of POSS, most have dealt with static structures and energies.[5,29−47] However, there is relatively little known about the dynamic behavior of the cage and the incompletely condensed silsesquioxanes. Answers to questions regarding the molecular size and shape, cavity dimensions, stability, and flexibility of the silsesquioxanes cage (**1**) and particularly the species generated when one (**2**, basket) and two (**3**, tube and **4**, ladder) siloxane units of the cage are opened are crucial in designing optimal catalysts that involve lipophilic bonding of the substrate. Toward this goal, we have used the Low Mode:Monte Carlo conformational search method to examine the conformational preference, stability, flexibility, and hydrophobicity of a series of oligomeric silsesquioxanes with R = OH and H in a vacuum and organic solvent ($CHCl_3$).

Methods

The conformational ensembles of **1**−**4** were calculated using version 8.1 of the MacroModel[48] suite of software programs running on 800 MHz Athlon PCs under the RedHat LINUX 6.2 operating system. Quantum calculations were performed with Jaguar V4.0.[49] The MM3 force field,[50] as implemented in MacroModel V8.1 (MM3*), was utilized along with the Generalized Born/Surface Area (GBSA) continuum model[51−56] for chloroform and water. The GBSA model has been shown

* Address correspondence to this author. E-mail: cparish@richmond.edu. Phone: (804) 484-1548. Fax: (804) 287-1897.
[†] Current address: Hobart and William Smith Colleges.
[‡] University of Richmond.

10.1021/jp052949j CCC: $30.25
Published on Web 08/30/2005

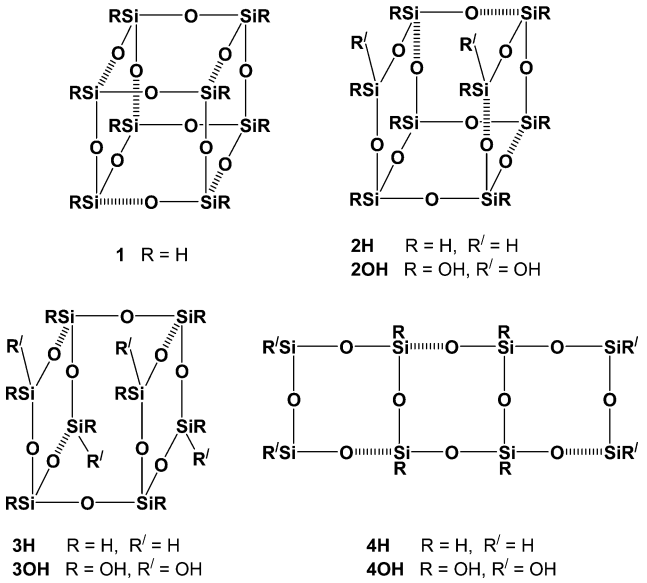

Figure 1. Polyhedral oligomeric silsesquioxane structures. Dashed lines indicate the bonds used during conformational searching to open the rings to allow for interconversion of ring conformations. All remaining bonds were included in the exploration of torsional space where each MC conformational search step varied a random number of torsional degrees of freedom between two and the maximum number of torsions available.

to reproduce solvation free energies obtained with the more elaborate Poisson−Boltzmann method and to determine hydration free energies to within 0.9 kcal/mol of experimental data for a series of compounds.[56] Moreover, the GBSA chloroform/water system has been shown to be a good model for estimating hydrophobicity.[57]

Conformational Searches. The Low Mode (LM) search method[58,59] was used in a 1:1 combination[60] with the Monte Carlo (MC) search method[61] to explore the potential energy surfaces of **1**−**4**. The conformational space of the ring moieties was sampled using the ring-opening method of Still[62] where the dashed lines in the molecules depicted in Figure 1 indicate the bonds that are broken to allow subsequent torsional rotation, which leads to interconversion of ring conformations. Each MC conformational search step varied a random number of torsional degrees of freedom between a minimum of two and the maximum number of torsions in each system. The total number of variable torsions in **1** is 19; **2H**, 18; **2OH**, 20; **3H**, 17; **3OH**, 21; **4H**, 17; and **4OH**, 21. LM frequencies corresponding to the 10 lowest eigenvectors were explored. The total traveling distance for each LM step was selected randomly between 3 and 6 Å. Searches were run in five blocks of 10 000 LM:MC steps. Convergence was judged by monitoring (a) the energy of the most stable structure, (b) the number of times this structure was visited, and (c) the number of unique conformations found within 50.0 kJ mol^{-1} of the lowest energy minimum. Unique conformations were determined by superimposition of all heavy (non-hydrogen) atoms as well as reflection and/or rotation of the atom-numbering scheme. Structures were considered to be duplicates and rejected if the maximum interatomic distance was 0.25 Å or less following optimal RMS superposition. Structures that were found in previous searches were used to seed subsequent searches. Searches utilized the usage-directed structure selection method[61] that identifies the least used structure from among all known conformations and then uses this structure as the starting point for each new search. This ensures that a variety of different starting structures from different regions of the potential energy surface are used to begin each new search. During the conformational search, all structures were subjected to 1500 steps of the Truncated Newton Conjugate Gradient (TNCG)[63] minimization method to within a derivative convergence criterion of 0.01 kJ $Å^{-1}$ mol^{-1}.

Clustering Ensembles. Ensembles generated for each of the structures were grouped into geometrically similar families using the XCluster[64] program. XCluster calculates the pairwise distance between each structure, in either torsional or Cartesian space, and partitions the conformations into geometrically similar subsets in an agglomerative, hierarchical fashion. The process begins with every structure as the only member of its own cluster. Individual structures are then grouped into clusters using the shortest distance between points as the threshold distance. At each clustering level the next shortest distance ($N - 1$) is used to form new, agglomerative clusters, with later clusters formed from groupings of earlier clusters. This process continues until all structures are a member of the same final cluster. The goal is to find the clustering level at which the distance between members of clusters is much smaller than the distance between clusters, i.e., the minimum separation ratio. It has been shown that separation ratios greater than two, which occur at high clustering levels, indicate significant clustering.[64] For a given clustering level, the full distance matrix was used to visualize the clustering of molecular structures in each ensemble. The clustering mosaics were used to illustrate how the clusters agglomerated as the clustering proceeded from the first level to the $N - 1$ level.

Results and Discussion

The conformational flexibility of the fully condensed POSS cage (**1**) and a variety of incompletely condensed structures (**2**−**4**) was investigated. Experimentally, one might envisage these POSS cages being opened via hydrolysis and, therefore, we chose to study systems in which the silicon atoms of the opened siloxane (Si−O−Si) bond were capped with hydroxyl groups. To ascertain the effect of the hydroxyl substitution on flexibility, we also studied the corresponding H-capped systems for comparison with the hydroxyl-capped molecules. For the incompletely condensed structures, one bond of **1** may be broken leading to a basket-like molecule substituted with two hydrogens or two hydroxyl groups on silicon (i.e., **2H** and **2OH**). Two bonds of **1** may also be broken leading to tube-like structures **3H** and **3OH** (breaking a bond at each of two diagonal edges of the cage) or ladder-like structures **4H** and **4OH** (breaking a bond on opposite edges of the same face).

Generating Potential Energy Surfaces. It is important to choose a force field that is well parametrized for the molecular system under study. Accurate torsional parameters are particularly important in flexible molecular systems since they control conformational interconversions. To our knowledge, most modeling studies of siloxane systems have utilized the MM2[65] force field due to its ability to reproduce accurately the experimental siloxane bond lengths, bond angles, and torsional barriers.[66−68] The MM2* and MM3* force fields, as implemented in the Batchmin program, are similar to but not identical with the originally published MM2 and MM3 force fields. The bond length, bond angle, and torsional equations are the same; however, the original MM2/MM3 dipole−dipole electrostatic description is replaced with partial charge electrostatics as derived from the original bond dipoles.

In this study, we had obtained with difficulty the energy-minimized ensembles for the hydroxyl-containing ladder structure, **4OH**, on the MM2*/GBSA($CHCl_3$) surface. Therefore, we performed a comparison of the MM2*, MM3*, and HF/6-31G**

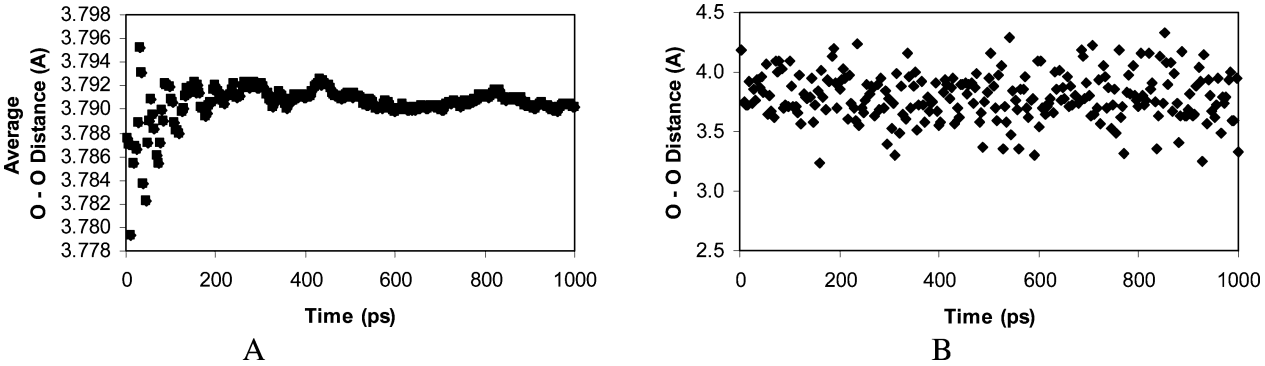

Figure 2. Molecular dynamics results for **1**: (A) Average O−O distance during 1000 ps MD simulation on the MM3*/GBSA($CHCl_3$) surface of **1** showing simulation convergence. (B) O−O distances sampled during the simulation.

TABLE 1: An Energetic Comparison of the Cage and Ladder Conformation of 4OH on the MM2*/GBSA($CHCl_3$), MM3*/GBSA($CHCl_3$), and HF/6-31G/SCRF(CCl_4) Surfaces**[a]

HF/6-31G**/ SCRF(CCl_4) rel energy (kJ mol^{-1})	MM3*/ GBSA($CHCl_3$) rel energy (kJ mol^{-1})	MM2*/ GBSA($CHCl_3$) rel energy (kJ mol^{-1})
14.2	29.6	56.3

[a] In all three cases the cage lies lower in energy than the ladder.

surfaces to determine whether MM3* would be a suitable replacement force field. The stretching, bending, and torsional parameters, as well as the partial charges, as determined by MM2* and MM3* for **4OH**, are quite similar.[69] A preliminary 5000 step search of **4OH** using the MM3* force field and the GBSA model for chloroform revealed that the lowest energy structure in the ensemble adopted a cage-like conformation while the 378th structure, some 29 kJ/mol higher in energy than the cage, appeared as the closest open, wavy ladder-like or S-shaped conformation. These two structures were subjected to a full energy minimization on the MM2*/GBSA($CHCl_3$) surface where the cage conformation lies 56.3 kJ/mol lower than the ladder conformation. The MM2* minimum energy structures are different from the MM3* structures (RMSD: cage = 0.66 Å; ladder = 1.03 Å); however, in each case the overall shape remains the same. The MM3* cage and ladder structures were subjected to a single point energetic analysis using HF/6-31G**/SCRF(CCl_4). On this surface the cage and ladder conformers of **4OH** are true energy minima as confirmed by a frequency analysis and the cage lies 14.2 kJ/mol lower than the ladder (Table 1). This analysis, along with a close comparison of the force field parameters, suggests that the MM3*/GBSA($CHCl_3$) surface is adequately representing systems **1**−**4**. In this study, we have used the LM:MC conformational search method on the MM3*/GBSA($CHCl_3$) surface to study the molecular behavior and flexibility of these systems.

How Rigid Is the Cage? Molecule **1** is often described as a "rigid" molecule. Not surprisingly, our conformational search results on the MM3*/GBSA($CHCl_3$) surface revealed a single structure after 50 000 search steps. Conformational searching methods provide enthalpic information about low energy structures whereas free energy methods provide enthalpic and entropic data, which are particularly useful when probing the flexibility of a single molecular conformation. Therefore, **1** was subjected to a 1000 ps molecular dynamics simulation at 300 K. The system was equilibrated for 100 ps and a 1.5 fs time step was used. Facial transannular O−O distances were monitored throughout the simulation and convergence was determined by monitoring the average O−O distance (Figure 2A) and the total energy. Throughout the simulation O−O distances of 3.2−4.3 Å were sampled. This corresponds to a 32.8−79.5 $Å^3$ cage cavity (Figure 2B); i.e., the cavity is large enough to accommodate small esters or hydrocarbons and, therefore, potentially serve as a lipophilic binding site. The O−O distances sampled in the MD simulation bracket nicely the high-level ab initio value of 3.726 Å determined previously[32] for this distance. Moreover, the conformational and MD results indicate that the POSS cage, while adopting only a single conformation, is able to undergo significant fluxional motion.

TABLE 2: LM:MC Conformational Search Results within a 50 kJ/mol Energetic Window above the Lowest Energy Structure for 2H and 2OH on the MM3*/GBSA($CHCl_3$) Surface

no. of steps	no. of conformations found	no. of lowest minimum visits	minimum energy (kJ/mol)
2H			
10 000	7	3608	−168.20
10 000	7	6593	−168.20
10 000	7	10078	−168.20
10 000	7	13670	−168.20
10 000	7	16745	−168.20
2OH			
10 000	28	1857	−270.96
10 000	28	3597	−270.96
10 000	28	5608	−270.96
10 000	28	7509	−270.96
10 000	28	9222	−270.96

What Is the Flexibility of the Basket (2H and 2OH)? Breaking one siloxane bond and capping the silicon atoms with hydrogen or hydroxyl groups leads to **2H** and **2OH**, respectively. The conformational flexibility of these systems was investigated using the LM:MC conformational search method (Table 2). Each search appeared convergent with respect to the number of structures found and the energy of the lowest conformer. This structure was frequently and increasingly revisited as the search continued providing evidence of a well-sampled surface. No new structures were found after the first block of 10 000 steps although each new block of searching begins at a new point on the potential energy surface. There were seven unique structures found on the H-capped surface of **2H** (Figure 3) and 28 on the hydroxylated surface of **2OH** (Figure 4). An inspection of these ensembles reveals that all minima on both surfaces correspond to a "cage-like" structure in agreement with experimental crystal structures of larger, but similarly incondensed systems.[25] The potential for an increase in flexibility caused by removing one corner of the silsesquioxane is offset by the rigidity of the remaining basket-like structure. The larger number of structures for the hydroxylated system corresponds to a simple "wagging" of the OH groups. The seven structures found for **2H** superimpose on the lowest energy structure with an average RMSD

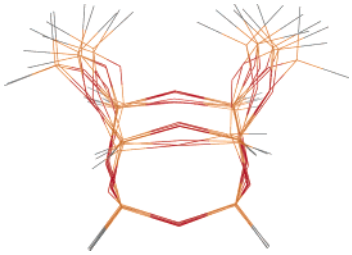

Figure 3. Superimposition of the seven low energy structures found on the MM3*/GBSA($CHCl_3$) surface of **2H**. Average RMSD from the lowest energy structure = 0.57 Å.

Figure 4. Superimposition of the 28 low energy structures found on the MM3*/GBSA($CHCl_3$) surface of **2OH**. Average RMSD from the lowest energy structure = 1.13 Å (all atoms) and 0.41 Å (ring atoms).

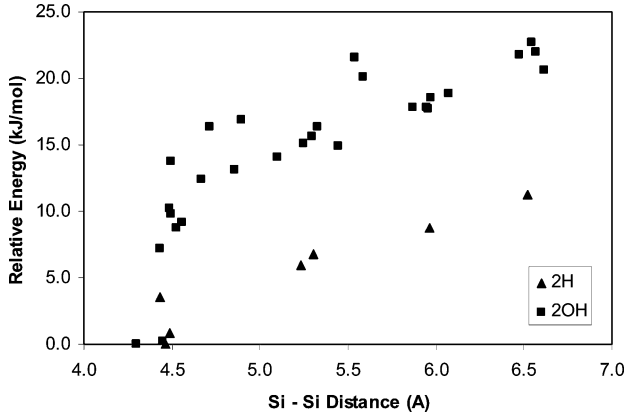

Figure 5. Relative energy versus cavity size for **2H** and **2OH**. The Si−Si distance corresponds to the distance between silicon atoms of the broken siloxane bond in the cage → basket conversion.

of 0.57 Å while the 28 structures of **2OH** superimpose onto their lowest energy structure with an average RMSD of 1.13 Å (all atoms) and 0.41 Å (ring atoms). The only major structural difference between conformations in each ensemble is the size of the cavity opening; that is, structures higher in energy exhibit larger openings and "bend open" or away from the cubic cage structure of the lowest energy conformation (Figures 3−5). The range in distances between the silicon atoms at the broken bond is approximately the same for both systems (4.2−6.5 Å); however, the energy range is about 15 kJ/mol greater for the hydroxylated system indicating an increase in ring strain energy induced by intramolecular hydrogen bonding among hydroxyl substituents.

Breaking Two Bonds. Breaking two bonds and capping the silicon atoms with an H or OH leads to two isomeric structures: a tube-like molecule formed by breaking two siloxane bonds on opposite diagonal edges of the cage (**3H**, **3OH)** and a ladder molecule formed by breaking two siloxane bonds on opposite edges of the same face (**4H**, **4OH)**. The lowest energy structures found after 10 000 conformational search steps are shown in Figure 6. In both the H-capped and OH-capped cases, the ladder isomer is more stable than the tube

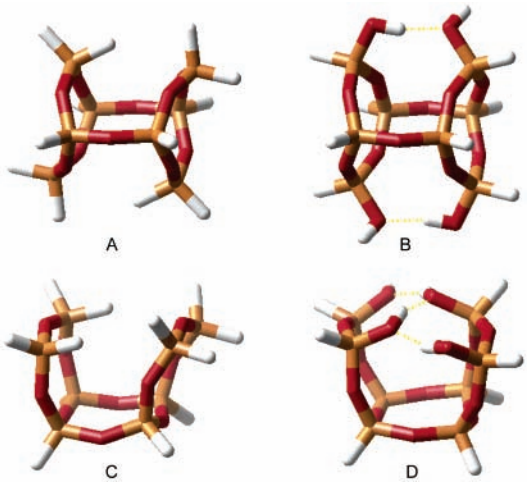

Figure 6. Lowest energy structures of **3H**, **3OH**, **4H**, and **4OH** found on the MM3*/GBSA($CHCl_3$) surface after 50 000 LM:MC conformational search steps. Hydrogen bonds between hydroxyl substituents are shown in yellow.

isomer: **4H** is 6 kJ/mol more stable than **3H** and **4OH** is 12 kJ/mol more stable than **3OH** on the MM3*/GBSA(CHCl3) surface.

The lowest energy structures of **3H** and **3OH** contain two eight-membered rings connected with two siloxane bridges. For each system both eight-membered rings adopt a boat-chair (BC) conformation using the nomenclature established by Hendrickson in his analysis of cyclooctane conformers.[70−73] More recently, Kolossvary and Guida[74] have shown that the BC conformer is the lowest energy cyclooctane conformer on the original MM2 surface. This agreement between the conformational energetic results for cyclooctane on the MM2 surface and for an eight-membered siloxane ring on the MM3* surface provides further indirect evidence for the quality of the MM3* treatment used in this study.

The lowest energy H-capped ladder structure, **4H**, retains the overall basket shape of the parent molecule **1**, while also adopting a BC conformation for one of the eight-membered rings and a chair-chair (or crown) (CC) conformation for the other two rings.[75] Similarly, the lowest energy OH-capped structure, **4OH**, retains the basket structure but contains all three rings in the CC conformation. The lowest energy structures of the hydroxylated systems are oriented optimally for hydrogen bonding, i.e., **3OH** contains two and **4OH** contains three such interactions. (Throughout this work, we will use the "classical" definition[76] of a hydrogen bond; a relaxation of these criteria to include more modern definitions of hydrogen bonding only increases the percentage of hydroxylated systems that display such behavior.) The conformational search results are shown in Tables 3 and 4.

Tube-like Structures (3H and 3OH). The LM:MC conformational search results for **3H** and **3OH** (Table 3) appear to be exhaustive as indicated by the convergence in the number of new structures found in the last 20 000 steps of sampling. There are 20 unique structures found on the MM3*/GBSA($CHCl_3$) surface of **3H**. These structures are very similar to the lowest energy minimum (Figure 6A) and superimpose onto this structure with an average RMDS of 0.68 Å. The ensemble of structures differs mainly in the conformations adopted by the eight-membered rings. Hendrickson[70−73] has shown that cyclooctane conformations can be classified into three families (BC, CC, and boat-boat, BB). The siloxane rings of the **3H** ensemble behave similarly and adopt all three of these confor-

TABLE 3: LM:MC Conformational Search Results within a 50 kJ/mol Energetic Window above the Lowest Energy Structure for 3H and 3OH on the MM3*/GBSA($CHCl_3$) Surface

no. of steps	no. of conformations found	no. of lowest minimum visits	minimum energy (kJ/mol)
3H			
10 000	20	970	−140.94
10 000	20	1950	−140.94
10 000	20	2697	−140.94
10 000	20	3670	−140.94
10 000	20	4604	−140.94
3OH			
10 000	573	56	−348.62
10 000	646	129	−348.62
10 000	666	200	−348.62
10 000	672	256	−348.62
10 000	672	318	−348.62

TABLE 4: LM:MC Conformational Search Results within a 50 kJ/mol Energetic Window above the Lowest Energy Structure for 4H and 4OH on the MM3*/GBSA($CHCl_3$) Surface

no of steps	no. of conformations found	no. of lowest minimum visits	minimum energy (kJ/mol)
4H			
10 000	143	135	−146.74
10 000	154	328	−146.74
10 000	141	491	−146.74
10 000	142	157	−146.74
10 000	142	827	−146.74
4OH			
10 000	2764	59	−360.36
10 000	3640	112	−360.36
10 000	4108	169	−360.36
10 000	4470	226	−360.36
10 000	4777	278	−360.36

mations as well as somewhat distorted or twisted variations on the theme. Another interesting feature of this ensemble is that there are 15 structures within 10 kJ/mol of the lowest energy structure and these all belong to the same conformational family; these 15 structures superimpose with an RMSD of 0.55 Å. The remaining five structures all lie within a range of 42.3 and 43.7 kJ/mol above the lowest energy minimum and contain an inverted silicon atom. This does not seem to be an artifact of the force field: a HF/6-31G** geometry optimization from the lowest energy MM3*/GBSA($CHCl_3$) structure (with an inverted silicon atom) relaxes to a very similar structure on the quantum surface that also contains an inverted silicon atom. This structure was confirmed to be a true minimum by frequency analysis and lies 42.5 kJ/mol higher than the structure that results from a HF/6-31G** geometry optimization starting from the MM3*/GBSA($CHCl_3$) lowest energy structure.

There are 672 unique minima within 50 kJ/mol of the lowest energy structure on the potential energy surface of **3OH**. This increase in the number of low energy minima for **3OH**, relative to the number found on the surface of **3H**, reflects the flexibility that arises from various low energy hydroxyl orientations and the significantly different low energy orientations under which intramolecular hydrogen bonding can take place. As with the **3H** ensemble, the **3OH** ensemble contains nine high energy structures (41.2 kJ/mol higher in energy) with inverted silicon atoms; however, there is no dramatic break in energy. The **3OH** ensemble contains structures with energies that smoothly increase from the lowest energy minimum to the highest energy structure found.

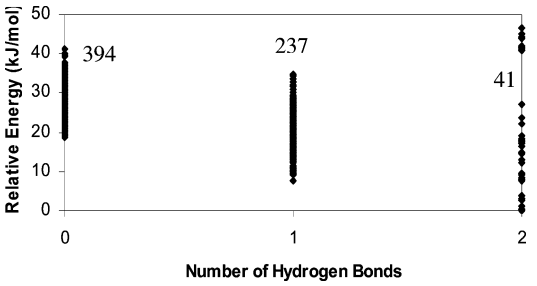

Figure 7. An analysis of the hydrogen-bonding behavior as a function of energy in the ensemble of structures for **3OH** found on the MM3*/GBSA($CHCl_3$) surface after 50 000 LM:MC conformational search steps. Of 672 structures in the ensemble, 394 structures contain zero, 237 structures contain one, and 41 structures contain two classically defined hydrogen bonds.

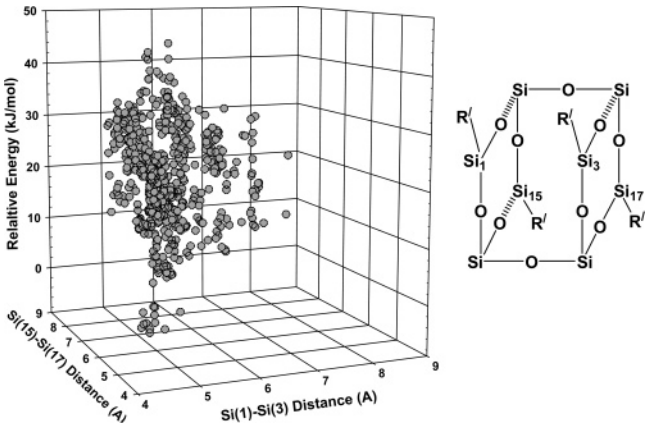

Figure 8. An analysis of the cavity opening as a function of energy in the ensemble of structures for **3OH** found on the MM3*/GBSA-($CHCl_3$) surface after 50 000 LM:MC conformational search steps. The graph demonstrates that the cavity size increases as the energy increases.

Clustering the minima found for **3OH** into conformational families yields further information about molecular flexibility. The XCluster program was used to determine if the ensembles naturally form structurally related groupings. Even with the inverted silicon atom in the highest nine structures, the **3OH** ensemble clusters into one family that is similar to the lowest energy structure shown in Figure 6B (average RMSD between the lowest energy minimum shown in Figure 6B and the 672 ensemble members = 1.4 Å). Within the **3OH** ensemble, 39% of the structures contain at least one hydrogen bond while 6% of the structures contain two hydrogen bonds; many of these conformations correspond to low energy structures (Figure 7). A structural examination of the ensemble for **3OH** (and **3H**, data not shown) indicates that structures higher in energy correspond to molecules with larger cavity openings (Figure 8).

Ladder-like Structures (4H and 4OH). Breaking two siloxane bonds on the same face of the cube leads to a ladder structure and provides the most flexible system in this study leading to the most diverse ensemble of structures. As shown in Figure 6C,D, the lowest energy structure of the ladder retains the overall cubic shape of a complete POSS cage and the lowest energy structure of **4OH** adopts a conformation that allows for optimal intramolecular hydrogen bonding. There are 142 structures found for **4H** and 4777 for **4OH**. The searches are convergent with respect to the energy and structure of the lowest minimum (Table 4).

Both of these ensembles cluster into two distinct families. At low energy the shape corresponds to the basket or cage-like structure of the lowest energy structure (Figure 9A). At higher

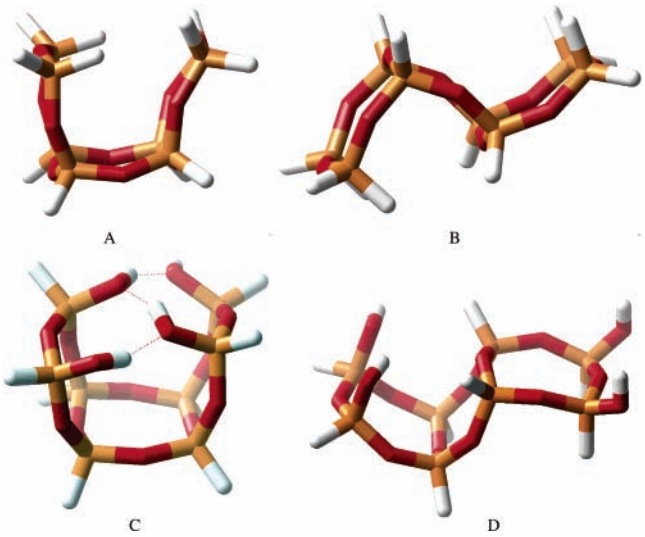

Figure 9. Representative structures from the two conformational families found for the ensemble of **4H** (A and B) and **4OH** (C and D). The lowest energy structure found for **4H** is the lead conformation in the cage-like family while structure no. 16 is the lead conformation for the S-shaped family. The lowest energy structure for **4OH** is the lead conformation in the cage-like family while structure no. 638 is the lead conformation for the S-shaped family.

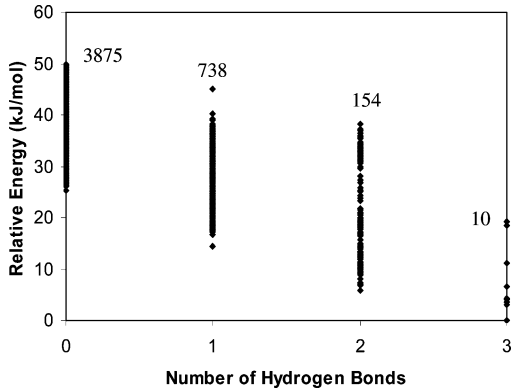

Figure 10. An analysis of the hydrogen-bonding behavior as a function of energy in the ensemble of structures for **4OH** found on the MM3*/GBSA($CHCl_3$) surface after 50 000 LM:MC conformational search steps. Of 4777 structures in the ensemble, 3875 structures contain zero, 738 structures contain one, 154 structures contain two, and 10 structures contain three classically defined hydrogen bonds.

energy the structures adopt a more open, "S"-like shape (Figure 9B). For **4H**, 44% of the ensemble retains the cage-like shape while 56% adopt more open conformations. The first nonbasket structure occurs at the 16th position in the ensemble: 3.18 kJ/mol higher in energy than the lowest energy minimum. For **4OH**, 55% of the structures are cage-like (Figure 9C) and 45% are S-like structures (Figure 9D). In this ensemble, the first non-cage-like structure occurs 29.1 kJ/mol higher in energy.

For **4OH**, a maximum of three hydrogen bonds are possible if the structure orients optimally as shown in the lowest energy structure (Figure 9C; dotted lines). As with **3OH**, the low energy structures of **4OH** are more likely to contain hydrogen bonds than the high energy structures, thereby revealing a tension between favorable intramolecular electrostatic interaction and steric strain (Figure 10). In the ensemble of structures for **4OH**, 10 conformations contain the maximum of three hydrogen bonds and these structures all lie within the lower energy regions of the ensemble.

Gas Versus Solvent Phase Behavior. Previous ab initio[5,29−41,77,78] and molecular modeling[43−47] studies of silsesquioxane systems have not included the effects of solvent. Bowers et al. found good agreement between their gas-phase molecular modeling results and experimental ion mobility measurements.[45] Of course, most routine uses of POSS systems, for instance as binding domains, would take place in the condensed phase. Therefore, we undertook a study of the flexibility of **1**−**4** in the gas phase in order to ascertain, by comparison, the role that solvent plays in the overall molecular behavior and flexibility. We include here results only for the most flexible system, **4OH**. Nevertheless, for all systems in this study the solvent ($CHCl_3$) and gas-phase behaviors are indistinguishable: the lowest energy structures are the same for hydrogen-capped systems (RMSD range 0.002−0.400 Å) and differ only in hydroxyl orientations for **2OH**, **3OH**, and **4OH**. In all cases, solvent lowers the energy of each system. For the hydroxylated systems we see an increase in the number of structures oriented optimally for hydrogen bonding, in the gas-phase relative to the solvent-phase, as would be expected. For instance, in the basket-shaped ensembles, **2OH**, only 11 of the lowest energy structures are oriented for hydrogen bonding in the solvent phase, but more than 50% of the structures (all at low energy) display hydrogen-bonding behavior in the gas-phase ensemble.

There are 4506 structures within 50 kJ/mol of the lowest energy minimum on the gas-phase MM3* potential energy surface of **4OH** compared to 4777 on the MM3*/GBSA($CHCl_3$) surface. The lowest energy structures on the surfaces are very similar and superimpose with an RMSD of 0.40 Å. The XCluster program was used to determine if the ensembles naturally form structurally related groupings and if the groupings are the same or different for each ensemble. Clustering the ensembles by superposition of all silicon and hydrogen ring atoms resulted in very strong and similar clustering. Both ensembles can be clustered (gas-phase separation ratio = 3.5; solvent-phase separation ratio = 3.3) into two conformational families with distinctly different representative structures that can be distinguished by their cage-like versus ladder-like or "S-shaped" conformations. The representative structure for each family on the gas-phase surface is very similar to the representative structures from the solvent surface shown in Figure 9C,D. The cage-like structure occurs 56% and 55% of the time and the ladder-like structure occurs 44% and 45% of the time in the gas- and solvent-phase ensembles, respectively. In both cases, the cage-like structure is found more often in the low energy regions while the ladder-like structure occurs with increasing frequency in the higher energy regions of the potential energy surface.

Aqueous Versus Organic Solvent-Phase Behavior. We find it particularly interesting that the slight polarity of the GBSA chloroform solvent medium does not affect the conformational flexibility of these systems, including the hydroxylated species. A comparison of the GBSA($CHCl_3$) results with the GBSA model for water provides further insight into the solubility properties of these systems. The GBSA energy has been previously shown[79] to be an accurate approximation for determining the free energy of solvation. With this in mind, the relative solvation free energies (SFE) of **1**−**4** in aqueous and nonaqueous ($CHCl_3$) environments were compared using the GBSA energy for each of the lowest energy minima found in this study (Table 5). The solvation free energies in chloroform are all negative and similar in magnitude, which indicates a favorable solubility in this solvent that is independent of structure, including the addition of hydroxyl groups. The aqueous solvation free energies vary significantly with structure,

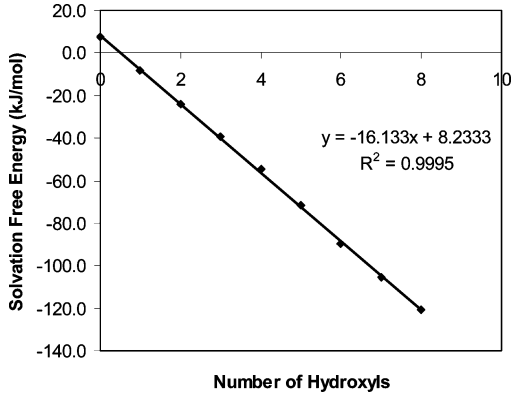

Figure 11. POSS hydration free energies as a function of hydroxyl substituents determined using the GBSA solvation model.

TABLE 5: Aqueous and Nonaqueous Solvation Free Energies Determined Using the GBSA Model for Water and Chloroform

	SFE (kJ/mol)	
structure	$CHCl_3$	H_2O
1	−28.9	7.6
2H	−29.8	9.0
2OH	−33.3	−13.4
3H	−30.8	10.2
3OH	−37.3	−23.7
4H	−30.6	10.4
4OH	−38.1	−34.3

i.e., the cage and hydrogen-substituted basket, ladder, and tube all have positive SFE values indicating a lack of solubility, while the hydroxyl substituted systems **2OH**, **3OH**, and **4OH** all have negative SFE values in the order basket < tube < ladder. From these results, it is a natural extension to assume that the aqueous solubility of the POSS cage, **1**, would improve with hydroxyl substitution. We used the GBSA solvent energies to explore the SFE values of **1** as a function of hydroxylation (Figure 11) and found that the aqueous solubility of the POSS cage increased linearly with the number of hydroxyl units decorating the surface. (For comparison, the GBSA energy of ethane is 7.1 kJ/mol; for ethanol the GBSA energy is −12.6 kJ/mol.)

Conclusions

The Low Mode:Monte Carlo conformational search method has been shown capable of exhaustively searching the MM3*/GBSA($CHCl_3$) surface of a polyhedral oligomeric silsesquioxane cage and related incompletely condensed systems and was used to identify the ensemble of all low lying structures. An energetic analysis indicated that there is a good correlation between points on the HF/6-31G**/solvent and MM3*/GBSA($CHCl_3$) surfaces. The cage molecule, **1**, exists as a single conformation that undergoes considerable breathing motion—enough to accommodate the binding of metal ions and small hydrocarbons. Breaking one siloxane bond does not alter the conformational behavior significantly; as might be expected there are a few more low energy structures (8 versus 1 for **2H** versus **1**); however, the overall cage-like shape is conserved in both the hydrogen- and hydroxyl-capped systems of **2**. Breaking two bonds leads to isomeric tube and ladder-like structures where the ladder isomer is lower in energy than the corresponding tube. There are numerous low energy structures on the hydrogen- and hydroxyl-capped tube MM3*/GBSA($CHCl_3$) surface; however, these structures cluster into one conformational family for which the cage-shaped lowest energy structure is representative. The ladder isomer is considerably more flexible than the tube isomer. Not only are there more low energy structures on the MM3*/GBSA($CHCl_3$) surface, but the conformations cluster into two different families: a cage-like family for which the lowest energy structure is representative and a more open, ladder-like structure. The low energy tube structures show a significant amount of intramolecular hydrogen bonding. Although more rigid than the ladder, the tube isomer appears to be better oriented to maximize this type of interaction relative to the ladder isomer. The conformational flexibility of **1**−**4** in the gas and solvent phase ($CHCl_3$) are very similar. Based on GBSA solvation energies for water and chloroform we expect that **1**−**4** will be soluble in organic solvents whereas only the hydroxylated systems will be soluble in water.

Acknowledgment is made to the donors of the Petroleum Research Fund, administered by the American Chemical Society, and the National Science Foundation under grant CHE-0211577 for partial support of this work. Undergraduate summer research stipends were also provided by grants from the Merck Foundation administered by the American Association for the Advancement of Science, the Patchett Family Foundation, and the Council on Undergraduate Research. Computational resources were provided in part by the MERCURY supercomputer consortium (http://mars.hamilton.edu) under NSF grant CHE-0116435.

References and Notes

(1) Davydov, V. Y. In *Adsorption on Silica Surfaces*; Papirer, E., Ed.; Marcel Dekker: New York, 2000.
(2) Impens, N. R. E. N.; van der Voort, P.; Vansant, E. F. *Microporous Mesoporous Mater.* **1999**, *28*, 217.
(3) Gorte, R. J. *Catal. Lett.* **1999**, *62*, 1.
(4) Clark, J. H. *Acc. Chem. Res.* **2002**, *35*, 791.
(5) Duchateau, R.; Dijkstra, T. W.; van Santen, R. A.; Yap, G. P. A. *Chem. Eur. J.* **2004**, *10*, 3979.
(6) Scott, D. W. *J. Am. Chem. Soc.* **1946**, *68*, 356.
(7) Feher, F.; Terroba, R.; Jin, R.-Z.; Wyndham, K. D.; Lucke, S.; Brutchey, R.; Nguyen, F. *Polym. Mater. Sci. Eng.* **2000**, *82*, 301.
(8) Li, G.; Wang, L.; Ni, H.; Pittman, C. U. J. *J. Inorg. Organomet. Polym.* **2001**, *11*, 123.
(9) Baney, R. H.; Itoh, M.; Sakakibara, A.; Suzuki, T. *Chem. Rev.* **1995**, *95*, 1409.
(10) Loy, D. A.; Shea, K. J. *Chem. Rev.* **1995**, *95*, 1431.
(11) Voronkov, M. G.; Lavrentyev, V. I. *Top. Curr. Chem.* **1982**, *102*, 199.
(12) Voronkov, M. G.; Lavrentyev, V. I.; Kovrigin, V. M. *J. Organomet. Chem.* **1981**, *220*, 285.
(13) Product Catalog, Hybrid Plastics, 2005 http://www.hybridplastics.com/catalog.htm.
(14) Lee, H.-J.; Goo, J.; Kim, S.-H.; Hong, J.-G.; Lee, H.-D.; Kang, H.-K.; Lee, S.-I.; Lee, M. Y. *Jpn. J. Appl. Phys., Part I* **2000**, *39*, 3924.
(15) Chaudhry, T. M.; Drzal, L. T.; Ho, H.; Laine, R. *Proc. Annu. Meet. Adhes. Soc.* **1996**, 126.
(16) Nakamatsu, K.-i.; Watanabe, K.; Tone, K.; Katase, T.; Hattori, W.; Ochiai, Y.; Matsuo, T.; Sasago, M.; Namatsu, H.; Komuro, M.; Matsui, S. *Jpn. J. Appl. Phys., Part I* **2004**, *43*, 4050.
(17) Duchateau, R. *Chem. Rev.* **2002**, *102*, 3525.
(18) Pescarmona, P. P.; Van der Waal, J. C.; Maschmeyer, T. *Chem. Eur. J.* **2004**, *10*, 1657.
(19) Pescarmona, P. P.; Masters, A. F.; Van der Waal, J. C.; Maschmeyer, T. *J. Mol. Catal.* **2004**, *220*, 37.
(20) Duchateau, R.; Dijkstra, T. W.; Severn, J. R.; van Santen, R. A.; Korobkov, I. V. *J. Chem. Soc., Dalton Trans.* **2004**, *17*, 2677.
(21) Kawasaki, T.; Ishikawa, K.; Sekibata, H.; Sato, I.; Soai, K. *Tetrahedron Lett.* **2004**, *45*, 7939.
(22) Wada, K.; Itayama, N.; Watanabe, N.; Bundo, M.; Kondo, T.; Mitsudo, T.-a. *Organometallics* **2004**, *23*, 5824.
(23) Al-Haq, N.; Ramnauth, R.; Kleinebiekel, S.; Ou, D. L.; Sullivan, A. C.; Wilson, J. *Green Chem.* **2002**, *4*, 239.
(24) Kudo, T.; Gordon, M. S. *J. Phys. Chem. A* **2003**, *107*, 8756.
(25) Gerritsen, G.; Duchateau, R.; van Santen, R. A.; Yap, G. P. A. *Organometallics* **2003**, *22*, 100.
(26) Rubinsztajn, S.; Zeldin, M.; Fife, W. K. *Macromolecules* **1991**, *24*, 2682.

(27) Fife, W. K.; Rubinsztajn, S.; Zeldin, M. *J. Am. Chem. Soc.* **1991**, *113*, 8535.
(28) Jackson, P.; Rubinsztajn, S.; Fife, W. K.; Zeldin, M.; Gorenstein, D. G. *Macromolecules* **1992**, *25*, 7078.
(29) Lin, T.; He, C.; Xiao, Y. *J. Phys. Chem. B* **2003**, *107*, 13788.
(30) Franco, R.; Kandalam, A. K.; Pandey, R.; Pernisz, U. C. *J. Phys. Chem. B* **2002**, *106*, 1709.
(31) Liu, L.-K.; Jiane-Bond, C.; Slanina, Z.; Chow, T. J. *J. Chin. Chem. Soc.* **2002**, *49*, 943.
(32) Tejerina, B.; Gordon, M. S. *J. Phys. Chem. B* **2002**, *106*, 11764.
(33) Cheng, W.-D.; Xiang, K.-H.; Pandey, R.; Pernisz, U. C. *J. Phys. Chem. B* **2000**, *104*, 6737.
(34) Mattori, M.; Mogi, K.; Sakai, Y.; Isobe, T. *J. Phys. Chem. A* **2000**, *104*, 10868.
(35) Uzunova, E. L.; St. Nikolov, G. *J. Phys. Chem. A* **2000**, *104*, 5302.
(36) Davidova, I. E.; Gribov, L. A.; Maslov, I. V.; Dufaud, V.; Niccolai, G. P.; Bayard, F.; Basset, J. M. *J. Mol. Struct.* **1998**, *443*, 89.
(37) Kudo, T.; Gordon, M. S. *J. Am. Chem. Soc.* **1998**, *120*, 11432.
(38) Xiang, K.-H.; Pandey, R.; Pernisz, U. C.; Freeman, C. *J. Phys. Chem. B* **1998**, *102*, 8704.
(39) Tossell, J. A. *J. Phys. Chem.* **1996**, *100*, 14828.
(40) Earley, C. W. *J. Phys. Chem.* **1994**, *98*, 8693.
(41) Calzaferri, G.; Hoffmann, R. *J. Chem. Soc., Dalton Trans.* **1991**, *S*, 917.
(42) Allen, E. C.; Beers, K. J. *Polymer* **2005**, *46*, 569.
(43) Baker, E. S.; Gidden, J.; Anderson, S. E.; Haddad, T. S.; Bowers, M. T. *Nano Lett.* **2004**, *4*, 779.
(44) Baker, E. S.; Gidden, J.; Fee, D. P.; Kemper, P. R.; Anderson, S. E.; Bowers, M. T. *Int. J. Mass Spectrom.* **2003**, *227*, 205.
(45) Gidden, J.; Kemper, P. R.; Shammel, E.; Fee, D. P.; Anderson, S.; Bowers, M. T. *Int. J. Mass Spectrom.* **2003**, *222*, 63.
(46) Bharadwaj, R. K.; Berry, R. J.; Farmer, B. L. *Polymer* **2000**, *41*, 7209.
(47) Park, S. S.; Xiao, C.; Hagelberg, F.; Hossain, D.; Pittman, C. U., Jr.; Saebo, S. *J. Phys. Chem. A* **2004**, *108*, 11260.
(48) Mohamadi, F.; Richards, N. G. J.; Guida, W. C.; Liskamp, R.; Lipton, M.; Caufield, C.; Chang, G.; Hendrickson, T.; Still, W. C. *J. Comput. Chem.* **1990**, *11*, 440.
(49) *Jaguar 4.0*, Schrodinger, L. L. C.: Portland, OR, 1991−2003.
(50) Allinger, N. L.; Yuh, Y. H.; Lii, J.-H. *J. Am. Chem. Soc.* **1989**, *111*, 8551.
(51) Weiser, J.; Shenkin, P. S.; Still, W. C. *J. Comput. Chem.* **1999**, *20*, 217.
(52) Weiser, J.; Shenkin, P. S.; Still, W. C. *J. Comput. Chem.* **1999**, *20*, 586.
(53) Weiser, J.; Weiser, A. A.; Shenkin, P. S.; Still, W. C. *J. Comput. Chem.* **1998**, *19*, 797.
(54) Hasel, W.; Hendrickson, T. F.; Still, W. C. *Tetrahedron Comput. Methodol.* **1988**, *1*, 103.
(55) Still, W. C.; Tempczyk, A.; Hawley, R. C.; Hendrickson, T. *J. Am. Chem. Soc.* **1990**, *112*, 6127.
(56) Qiu, D.; Shenkin, P. S.; Hollinger, F. P.; Still, W. C. *J. Phys. Chem. A* **1997**, *101*, 3005.
(57) Reynolds, C. H. *J. Chem. Inf. Comput. Sci.* **1995**, *35*, 738.
(58) Kolossvary, I.; Guida, W. C. *J. Comput. Chem.* **1999**, *20*, 1671.
(59) Kolossvary, I.; Guida, W. C. *J. Am. Chem. Soc.* **1996**, *118*, 5011.
(60) Parish, C.; Lombardi, R.; Sinclair, K.; Smith, E.; Goldberg, A.; Rappleye, M.; Dure, M. *J. Mol. Graphics Modell.* **2002**, *21*, 129.
(61) Chang, G.; Guida, W. C.; Still, W. C. *J. Am. Chem. Soc.* **1989**, *111*, 4379.
(62) Still, W. C.; Galynker, I. *Tetrahedron* **1981**, *37*, 3981.
(63) Ponder, J. W.; Richards, F. M. *J. Comput. Chem.* **1987**, *8*, 1016.
(64) Shenkin, P. S.; McDonald, D. Q. *J. Comput. Chem.* **1994**, *15*, 899.
(65) Allinger, N. L. *J. Am. Chem. Soc.* **1977**, *99*, 8127.
(66) Grigoras, S.; Lane, T. H. *J. Comput. Chem.* **1988**, *9*, 25.
(67) Grigoras, S.; Lane, T. H. Conformational analysis of substituted polysiloxane polymers. In *Advances in Chemistry Series 224*: *Silicon-Based Polymer Science A Comprehensive Resource*; Zeigler, J. M., Fearon, F. W. G., Eds.; American Chemical Society: Washington, DC, 1990; p 127.
(68) Bahar, I.; Zuniga, I.; Dodge, R.; Mattice, W. L. *Macromolecules* **1991**, *24*, 2986.
(69) The MM2 and MM2* force fields contain lone pairs on oxygen. The stretching, bending, and torsional parameters, as well as the partial charges, determined by MM2* and MM3* for **4OH** are quite similar if the difference in lone pair treatment is taken into account.
(70) Hendrickson, J. B. *J. Am. Chem. Soc.* **1961**, *83*, 4537.
(71) Hendrickson, J. B. *J. Am. Chem. Soc.* **1964**, *86*, 4854.
(72) Hendrickson, J. B. *J. Am. Chem. Soc.* **1967**, *89*, 7047.
(73) Hendrickson, J. B. *J. Am. Chem. Soc.* **1967**, *89*, 7036.
(74) Kolossvary, I.; Guida, W. C. *J. Am. Chem. Soc.* **1993**, *115*, 2107.
(75) On the MM2* surface the BC conformation is 11 kJ/mol more stable than the CC conformation.
(76) Steiner, T. *Angew. Chem., Int. Ed.* **2002**, *41*, 48.
(77) Kudo, T.; Gordon, M. S. *J. Phys. Chem. A* **2002**, *106*, 11347.
(78) Kudo, T.; Gordon, M. S. *J. Phys. Chem. A* **2000**, *104*, 4058.
(79) Reddy, R. M.; Erion, M. D.; Agarwal, A.; Viswanadhan, V. N.; McDonald, Q. D.; Still, W. C. *J. Comput. Chem.* **1998**, *19*, 769.